THE JOURNAL OF PHYSICAL CHEMISTRY Letters

Letter

pubs.acs.org/JPCL

Quantum Nonlinear Optics with Polar J-Aggregates in Microcavities

Felipe Herrera,*[,†] Borja Peropadre,[†] Leonardo A. Pachon,[†,‡] Semion K. Saikin,[†,¶] and Alán Aspuru-Guzik*[,†]

[†]Department of Chemistry and Chemical Biology, Harvard University, Cambridge, Massachusetts 02138, United States

[‡]Grupo de Física Atómica y Molecular, Instituto de Física, Facultad de Ciencias Exactas y Naturales, Universidad de Antioquia UdeA, Calle 70 No. 52-21, Medellín, Colombia

[¶]Institute of Physics, Kazan Federal University, 18 Kremlevskaya Street, Kazan 420008, Russian Federation

Supporting Information

ABSTRACT: We predict that an ensemble of organic dye molecules with permanent electric dipole moments embedded in a microcavity can lead to strong optical nonlinearities at the single-photon level. The strong long-range electrostatic interaction between chromophores due to their permanent dipoles introduces the desired nonlinearity of the light−matter coupling in the microcavity. We develop a semiclassical model to obtain the absorption spectra of a weak probe field under the influence of strong exciton−photon coupling with the cavity field. Using realistic parameters, we demonstrate that a cavity field with an average photon number near unity can significantly modify the absorptive and dispersive response of the medium to a weak probe field at a different frequency. Finally, we show that the system is in the regime of cavity-induced transparency with a broad transparency window for dye dimers. We illustrate our findings using pseudoisocyanine chloride (PIC) J-aggregates in currently available optical microcavities.

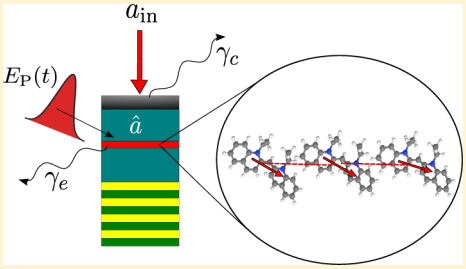

SECTION: Physical Processes in Nanomaterials and Nanostructures

J-aggregates[1−5] are arrays of dye molecules with large dipole moments that exhibit strong intermolecular electrostatic interaction, giving rise to collective effects in their coupling with electromagnetic fields. The specific set of linear and nonlinear optical properties of J-aggregates has stimulated a resurgence of interest in them for applications in modern photonics. A large linear absorption cross section combined with a narrow line width[6] at room temperatures make J-aggregates attractive for the design of optical processing devices operating at low light levels. J-aggregates can be readily coupled to solid-state photonic[7,8] and plasmonic[9−11] structures, extending the conventional photonics to subdiffraction length scales.[5] Illustrative examples of molecule-based photon processing structures can be found in nature, where photosynthetic organisms use molecular aggregates to collect light and deliver the photon energy on the scale of tens of nanometers.[12]

Moderately strong laser fields are commonly used to observe coherent optical phenomena in atomic gases and a few solid-state systems characterized by long dephasing times exceeding milliseconds at room temperature.[13−15] Solid-state semiconducting materials have much shorter electronic coherence times on the order of hundreds of femtoseconds, which greatly increases the laser intensity required to induce coherent optical phenomena in free space. For instance, in order to observe electromagnetically induced transparency (EIT) using inorganic quantum dots with terahertz dephasing rates, the required control laser intensity should be on the order of tens of MW/cm^2.[16] The same applies for organic materials, including J-aggregates. Such high intensities can optically damage an organic medium.[17] It is therefore necessary to replace the control lasers by the strong electric field per photon achievable in photonic structures[5] in order to observe coherent optical response with organic matter at room temperature.

Experimental progress in the fabrication of organic optical microcavities has demonstrated the ability to strongly couple an ensemble of organic chromophores with the confined electromagnetic field of a cavity mode at room temperature,[7,18−22] via the emergence of polariton modes in the cavity transmission spectra. The strong coupling of organic ensembles with plasmonic modes has also been demonstrated.[5,9,23−26] Moreover, the regime of ultrastrong coupling with organic molecules is now within reach, where the light−matter interaction energy reaches a significant fraction of the associated transition frequency.[27] These experimental advances enable the possibility of understanding and possibly manipulating the excited-state dynamics of molecular aggregates using a small number of photons.

In this Letter, we address the question whether collective multiexciton states in J-aggregates can be exploited for the coherent control of confined optical fields in photonic structures. In order to achieve this, we extend the nonlinear exciton equation (NEE) formalism[28,29] to account for the

Received: September 8, 2014
Accepted: October 7, 2014

   dx.doi.org/10.1021/jz501905h | J. Phys. Chem. Lett. 2014, 5, 3708−3715

nonperturbative coupling of the medium to a confined optical field. The active medium under consideration consists of an ensemble of one-dimensional polar J-aggregate domains embedded in an optical microcavity, as shown in Figure 1a.

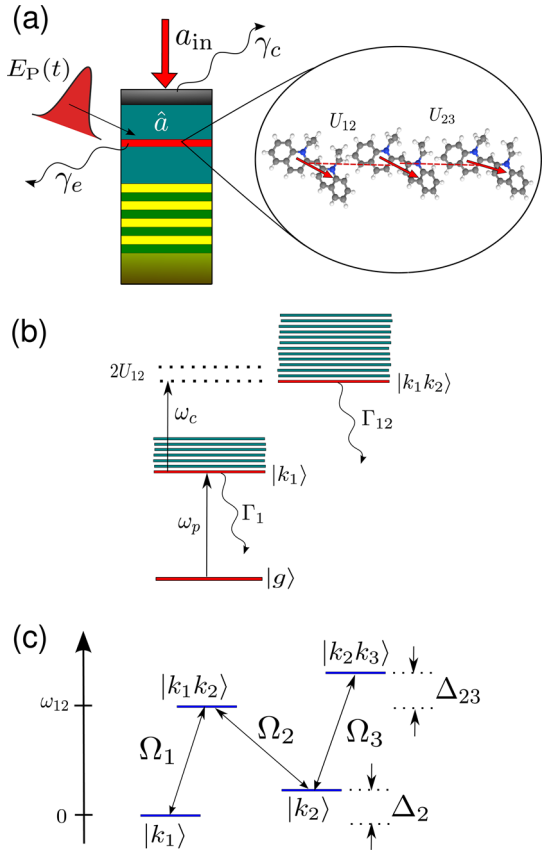

Figure 1. (a) Illustration of an optical microcavity containing an ensemble of two-dimensional J-aggregates. The cavity mode a_c is driven by a weak input field a_{in} and decays through the semireflecting mirror at the rate γ_c. A weak probe field at frequency $\omega_p > \omega_c$ couples directly to the organic chromophores. Individual molecules decay into external modes with a rate γ_e. Dipole−dipole interactions between individual chromophores in each aggregate modify the single-molecule response of the medium to the cavity and probe fields. (b) Energy spectrum of an individual aggregate showing the one-exciton and two-exciton bands (bandwidths not on scale). The cavity field drives all of the allowed coherences between states $|k_i\rangle$ and $|k_ik_j\rangle$, and the weak probe removes population from the ground state $|g\rangle$. The transition frequency between $|k_i\rangle$ and $|k_ik_j\rangle$ is shifted by the interaction energy $\sim U_{ij}$ with respect to the noninteracting case. (c) Effective four-level system coupled by the cavity with Rabi frequencies $\Omega_2 > \Omega_1 > \Omega_3$. The cavity frequency ω_c is assumed to be near-resonance with the transition $|k_1\rangle \rightarrow |k_2\rangle$. This model is used in eq 8 to describe the probe absorption at frequency $\omega_p < \omega_c$.

Each aggregate chain consists of a large number of polar organic dyes, such as pseudoisocyanine chloride (PIC), coupled to each other via dipole−dipole interactions. Interactions due to transition dipole moments lead to the formation of delocalized excitonic modes, represented as $|k_i\rangle$ in Figure 1b. The presence of permanent dipole moments both in the ground and excited molecular states leads to the emergence of exciton−exciton interactions, denoted as U_{ij} in Figure 1b, which shifts the energy of two-exciton states $|k_ik_j\rangle$ with respect to the case of nonpolar molecules. Each molecular aggregate is coupled to two light fields, a microcavity field of frequency ω_c with a large electric field per photon due to micron-size confinement and an external weak probe field of frequency ω_p that is far-detuned from the (lowest) cavity resonance frequency by an amount comparable to U_{ij} but nevertheless propagates inside of the microcavity due to the finite transmittivity of the upper lossy mirror.

We wish to exploit the organic medium as a nonlinear optical material with a large optical response at low light levels. In particular, we want to demonstrate that by exploiting the strong dipole−dipole interaction between individual chromophores due to their permanent dipoles, plus the strong collective coupling of a molecular aggregate with the cavity field, it is possible to perform light-by-light switching at the single-photon level. In this Letter, we develop a semiclassical model to predict that the presence of a single photon (on average) at the cavity frequency can modify absorptive and dispersive response of the organic medium to a weak external probe at a different frequency. The intermolecular electronic coupling between chromophores is responsible for establishing the required anharmonicities in the material spectrum, and the large electric field per photon of the confined cavity mode reduces the number of control photons required to achieve an observable switching effect. The model is semiclassical in the sense that we neglect, for simplicity, all quantum correlations between the cavity mode and the J-aggregates. However, we need to consider the quantized nature of the cavity and probe fields due to the low mean photon numbers (less than two) involved in the scheme.

To describe the evolution of the medium polarization $\mathbf{P}(t)$, we employ a quantum Langevin formalism. The key features of our model are (i) the strong coupling of the molecular ensemble with the cavity field and (ii) the intermolecular resonant energy tranfer via transition dipoles, known as Förster coupling J_{ij}, in addition to diagonal dipole−dipole interaction U_{ij} via permanent dipoles. Additionally, we consider chromophore relaxation due to spontaneous emission outside of the confined cavity mode, coupling of the chromophores to a phonon bath, and inhomogeneous broadening due to static disorder in chromophore transition energies. The evolution of an observable O in the Heisenberg picture is given by $\mathrm{d}O/\mathrm{d}t = -\mathrm{i}[O, \mathcal{H}_S + \mathcal{H}_{SB}]$ (we use $\hbar = 1$ throughout), where the Hamiltonian $\mathcal{H}_S$ describes the coherent evolution of the system degrees of freedom and $\mathcal{H}_{SB}$ the interaction of the system with the environment. More specifically, $\mathcal{H}_S$ describes the interaction of a single planar J-aggregate containing N chromophores with the electromagnetic field of a single cavity mode at frequency ω_c as well as a probe field at frequency ω_p and can be partitioned as

$$\mathcal{H}_S = H_1 + H_2 + H_3 \tag{1}$$

The first term describes a single effective molecular aggregate, as defined in the Supporting Information (SI), in the one-exciton eigenbasis as

$$H_1 = \sum_k \omega_k B_k^\dagger B_k + \sum_{kp} U_{kp} B_k^\dagger B_p^\dagger B_k B_p \tag{2}$$

The bosonic operator B_k annihilates an exciton in the kth mode, with $k = \{1, 2, ..., N\}$. We assume that the aggregate is a collection of two-level chromophores, with ground state $|g\rangle$ and excited state $|e\rangle$ having a site-dependent transition energy $\varepsilon_i = \omega_e + d_i$, where d_i is a small random shift from the gas-phase transition frequency ω_e that models structural or so-called static

dx.doi.org/10.1021/jz501905h | J. Phys. Chem. Lett. 2014, 5, 3708−3715

disorder.[30,31] The first term in eq 2 is the diagonal form of the site-basis Frenkel exciton Hamiltonian $H_0 = \sum_i \varepsilon_i B_i^\dagger B_i + \sum_{ij} J_{ij} B_i^\dagger B_j$. We take the electrostatic interaction between molecules as purely classical. In the point dipole approximation, the exchange coupling energy is $J_{ij} = (1 - 3\cos^2\Theta_{ij}) d_{eg}^2 / r_{ij}^3$, where Θ_{ij} is the angle between the transition dipole moments d_{eg} of molecules i and j (assumed parallel) and the intermolecular separation vector $\mathbf{r}_{ij} = r_{ij}\mathbf{r}_{ij}$. The second term in eq 2 describes the interaction between two exciton eigenstates due to long-range forces between the permanent dipoles of the chromophores. Here, we assume a simplified form of the scattering potential $U_{kp} = \sum_{ij} U_{ij} |c_{ik}|^2 |c_{jp}|^2$, where c_{ik} is an element of the unitary transformation $B_i = \sum_k c_{ik} B_k$. The interaction energy between sites is $U_{ij} = (1 - 3\cos^2\Theta_{ij})(\Delta d)^2 / r_{ij}^3$, where $\Delta d = d_e - d_g$ is the change in permanent dipole moment upon excitation of the chromophores.[32] For homogeneous aggregates, large values of U_{12} can lead to the formation of biexcitons with a binding energy proportional to U_{12}.[32] In this work, we simplify the two-exciton problem by assuming that the leading effect of the potential U_{kp} is to red shift or blue shift the two-exciton band with respect to the noninteracting case, for attractive or repulsive interactions, respectively. For simplicity, we take two-exciton eigenstates as direct products of single-exciton states.

The second term $H_2 = \omega_c a^\dagger a + \omega_p \mathcal{E}^\dagger \mathcal{E}$ in eq 1 is the free Hamiltonian for the cavity and probe fields, and the third term describes light−matter interaction as

$$H_3 = \mathrm{i} \sum_k g_k(t)(\mathcal{E}^\dagger B_k - B_k^\dagger \mathcal{E}) + \mathrm{i} \sum_{kq} D_{k,kq}(a^\dagger B_k^\dagger B_k B_q - B_q^\dagger B_k^\dagger B_k a) \tag{3}$$

where $g_k(t) = (N_A)^{1/2}(\vec{\mu}_k \cdot \mathbf{e}_p) E_p(t)$ is proportional to the single-exciton transition dipole moment $\vec{\mu}_k = \langle k|\vec{\mu}|g\rangle$ and $D_{k,kq} = (N_A)^{1/2}(\vec{\mu}_{k,kq} \cdot \mathbf{e}_c)\mathcal{E}_c$ is proportional to the one-to-two-exciton transition dipole moment $\mu_{k,kq} = \langle k|\vec{\mu}|kq\rangle$. We assume that the cavity supports a single mode with transverse polarization that is near-resonance with the strongest one- to two-exciton transition. Higher-frequency modes are assumed to be far-detuned and thus ignored. The organic medium typically consists of an ensemble of aggregate domains.[3,33] Within each domain, the intermolecular interactions are much stronger than those between domains. For simplicity, we idealize the medium by assuming that each domain contains a single one-dimensional aggregate, and all domains are identical. N_A is the number of aggregates in the medium (details in the SI). $E_p(t)$ and $\mathbf{e}_p$ are the electric field envelope and polarization of the probe. $\mathcal{E}_c$ is the electric field per cavity photon and $\mathbf{e}_c$ its polarization. The probe and cavity polarizations are assumed to be collinear. Each molecular aggregate interacts simultaneously with the cavity and probe fields. In eq 3, we assume that the probe and cavity fields do not drive the same transitions. In reality, both fields interact with all allowed transitions, but we neglect off-resonant contributions to the light−matter coupling.

The system−bath interaction is partitioned as $\mathcal{H}_{SB} = H_{ex} + H_{cav}$, where H_{cav} describes the decay of the cavity mode through the mirror of a one-sided microcavity, which corresponds to a typical experimental setup.[17] The term H_{ex} describes the radiative decay of excitons into electromagnetic modes outside of the cavity in addition to dephasing of excitons via interactions with phonons. The specific form $\mathcal{H}_{SB}$ and the relaxation tensors for system observables used in this work are given in the SI.

We are interested in the polarization $\mathbf{P}(t)$ of the medium, induced by the weak coherent probe field $\mathcal{E}$, with frequency ω_p. The medium polarization at frequency ω_p is given by

$$\mathbf{P}(t) = \sum_k \mu_k \{\langle B_k(t)\rangle + \langle B_k^\dagger(t)\rangle\} \tag{4}$$

We therefore need to solve the quantum Langevin equation for the exciton coherence in the steady state $\langle B_k(t \to \infty)\rangle$. The nonlinearity in the system Hamiltonian H_1 in eq 1 couples the observable B_k with an infinite hierarchy of equations of motion involving powers of the material operators B_k and $B_k^\dagger$. Because we are interested in the interaction of the medium with at most one probe photon and one cavity photon on average, we invoke a dynamics-controlled truncation scheme (DCT)[34] to truncate the hierarchy at third order, thus neglecting correlation functions involving products of four or more excitonic variables in the equations of motion. Given the small excitation density generated by the weak probe, we also assume that the ground-state population remains near unity at all times, ignoring contributions from density terms such as $\langle B_k^\dagger B_k\rangle$ in the equations of motion. Moreover, we assume a semiclassical approximation for the cavity field, which amounts to factorizing the correlation functions involving products of cavity and material variables. The dynamics of the medium polarization is thus governed by the equations

$$\frac{\mathrm{d}}{\mathrm{d}t}\langle B_k\rangle = \left(-\mathrm{i}\omega_k - \frac{\Gamma_k}{2}\right)\langle B_k\rangle - g_k\langle\mathcal{E}\rangle + \sum_{pq} D_{k,pq}\langle a^\dagger\rangle\langle B_p B_q\rangle \tag{5}$$

$$\frac{\mathrm{d}}{\mathrm{d}t}\langle B_p B_q\rangle = [-\mathrm{i}(\omega_p + \omega_q + 2U_{pq}) - \Gamma_{pq}]\langle B_p B_q\rangle - 2\sum_k D_{k,pq}\langle B_k\rangle\langle a\rangle - (g_p\langle B_q\rangle + g_q\langle B_p\rangle)\langle\mathcal{E}\rangle \tag{6}$$

Assuming that the phonon and the photon baths are Markovian, the Langevin noise terms in the equations of motion do not contribute to the evolution of the expectation values $\langle B_k\rangle$ and $\langle a\rangle$.[35] For simplicity, we have also neglected the effect of Langevin noise terms in the two-point and three-point correlation functions. For the validity of the semiclassical cavity regime, we assume that the cavity mode is weakly driven by a coherent field with $\langle a_{in}\rangle > 0$ in the underdamped regime. We have ignored contributions of three-point correlation functions of the form $\langle B_p^\dagger B_q B_k\rangle$, representing one-to-two exciton coherences. These coherence can be shown to remain negligible unless the ground state is depleated by the probe field beyond the perturbative regime. The cavity field couples directly to the $\langle B_p^\dagger B_q B_k\rangle$ in the Langevin equations (see the SI). Therefore, in the perturbative regime with respect to the probe field, the cavity amplitude $\langle a(t)\rangle$ evolves as if the cavity was empty. In other words, the cavity field does not undergo Rabi oscillations.

Despite the number of simplifications made in the derivation of eqs 5 and 6, we note that they have the same structure as the NEE that Chernyak et al.[28,29] derived by taking into account the nonboson commutation of exciton operators, density terms, and inelastic exciton−exciton scattering. Therefore, on the basis of several previous studies of nonlinear optical spectroscopy

dx.doi.org/10.1021/jz501905h | J. Phys. Chem. Lett. 2014, 5, 3708−3715

using the NEE in the regime of perturbative light−matter interaction,[29] we expect our model to provide an accurate qualitative description of the nonlinear response of molecular aggregates in microcavities where the coupling to the cavity mode is nonperturbative.

We are interested in the steady-state response of the system to the probe field for time scales long compared with the exciton and cavity lifetimes. Moreover, we assume that the cavity field decays at a rate slower than the exciton coherence decay ($1/\Gamma_k \approx 10^2$ fs), which does not require very high Q cavities at room temperature.[17] This separation of time scales allows us to solve eqs 5 and 6, taking the cavity and probe amplitudes as constants. Another important assumption in our model is the resolution of frequencies in the system. We require the detuning of the probe field from the cavity field $\delta = \omega_c - \omega_p$ to be larger than the exciton line width. In the SI, we show that under such assumptions, we can use eqs 5 and 6 to write the steady-state probe susceptibility as $\epsilon_0\chi(\omega_p) = \sum_k \mu_k X_k / i\mathcal{E}_p$, where $\mu_k \equiv (\vec{\mu}_k \cdot \mathbf{e}_p)$ and the one-exciton coherences $\mathbf{X} = [X_1, X_2, ..., X_N]^T$ are obtained by solving the linear system

$$\mathbf{MX} = \mathbf{B} \tag{7}$$

where the matrix $\mathbf{M} = (\mathbf{O} + 2|A_c|^2\mathbf{T})$ encodes the relevant light−matter interaction parameters in the one-photon and two-photon detuning matrixes $\mathbf{O}$ and $\mathbf{T}$, respectively, and $A_c \equiv \langle a \rangle$ is the mean cavity amplitude. The vector $\mathbf{B} = [\mu_1, \mu_2, ..., \mu_N]^T$ contains the one-exciton transition dipole moments. The definition of the matrices $\mathbf{O}$ and $\mathbf{T}$ can be found in the SI.

In the adopted semiclassical regime, the absence of the cavity is defined as $A_c = 0$, where the linear response is simply given by a sum of Lorentzians centered at the exciton frequencies ω_k, weighted by the corresponding transition dipole moments g_k. The coupling to the cavity therefore modifies the absorptive and dispersive response of the medium to the weak probe, as described below. We note that the aggregate absorption spectra obtained from eq 7 satisfies the sum rule $\int \mathrm{Im}[\chi(\omega_p)]\, d\omega_p = N\pi/\epsilon_0$ for all values of A_c.

In order to illustrate the developed model in eq 7, we calculate the probe susceptibility $\chi(\omega_p)$ for open one-dimensional homogeneous J-aggregates of size N. In Figure 2, we show the computed absorption probe spectra for PIC J-aggregates with $N = 100$ and 6. We use the transition energy $\omega_e = 2.25$ eV for all sites, nearest-neighbor excitonic coupling $J_{12} = -68.2$ meV, and dipole−dipole coupling $U_{12} = -198$ meV. These parameters were obtained by Markov et al.[36] from the observation of a red-shifted induced absorption peak in the pump−probe spectra of PIC aggregates. The relaxation tensors Γ_k and Γ_{pq} are dominated by phonon scattering (see SI), and for simplicity, we set $\Gamma_k = \Gamma_{pq} \approx 26$ meV, which gives a lower bound for the exciton dephasing rate at room temperature.[37] The vacuum Rabi frequency in microcavities can reach values on the order of $\Omega_c \approx 100$ meV.[7] In Figure 2, we set the vacuum Rabi frequency $\Omega_c \equiv (N_A)^{1/2}\langle e|\vec{\mu}\cdot\mathbf{e}_c|g\rangle\mathcal{E}_c = \Gamma_k$ so that $D_{k,kp} \approx N^{1/2}\Omega_c$ for the strongest excitonic transitions exceeds the dissipation rates, as is required in the strong coupling regime.

The probe absorption spectra in Figure 2a display a four-peak structure where the peak splitting scales linearly with the mean cavity amplitude A_c. The free-space spectrum corresponds to the J-band without static disorder. The peak splitting trend with increasing A_c can be qualitatively explained using a semiclassical model in which a classical cavity field of frequency ω_c couples strongly with two states in the one-exciton band (labeled $|k_1\rangle$ and $|k_2\rangle$) and two states in the two-exciton band

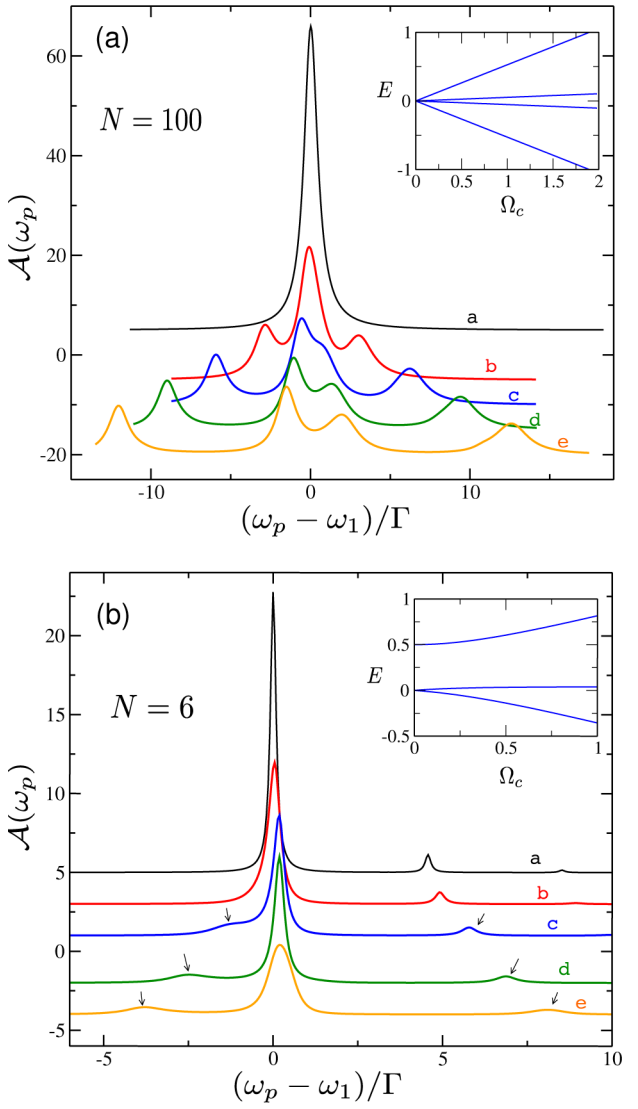

Figure 2. Probe absorption spectrum $\mathcal{A}(\omega_p) = -\mathrm{Im}[\chi]$ (in units of $\epsilon_0/\hbar$) as a function of the detuning from the lowest exciton resonance $\Delta_1 = \omega_p - \omega_1$ (in units of the decay rate $\Gamma = 26$ meV) for an ideal open linear polar J-aggregate of size N in a microcavity (no energetic disorder). (a) $N = 100$. Curves are labeled according to the mean cavity amplitude $A_c \equiv |\langle a \rangle|$ as (a) no cavity, (b) $A_c = 0.2$, (c) $A_c = 0.4$, (d) $A_c = 0.6$, and (e) $A_c = 0.8$. The inset shows the eigenvalues of the four-level effective Hamiltonian in eq 8 with $\Delta_2 = 0 = \Delta_{23}$ and $\Omega_1 = \Omega_2/3 = 3\Omega_3$ as a function of $\Omega_c = \Omega_2$ (in arbitrary units). (b) $N = 6$. Curves are labeled by the value of A_c as (a) no cavity, (b) $A_c = 0.4$, (c) $A_c = 0.8$, (d) $A_c = 1.2$, and (e) $A_c = 1.6$. The inset shows the eigenvalues of eq 8 with $\Delta_2 = 0.5$, $\Omega_1 = \Omega_2/3$, and $\Omega_3 = 0$ as a function of $\Omega_c = \Omega_2$. In both panels, the cavity frequency is resonant with the transition $|k_1\rangle \rightarrow |k_1k_2\rangle$.

($|k_1k_2\rangle$ and $|k_2k_3\rangle$). The coupling scheme is illustrated in Figure 1c. The transition dipole moments from the ground state $|g\rangle$ to the states $|k_1\rangle$, $|k_2\rangle$, and $|k_3\rangle$ have the largest values in the one-exciton band and satisfy $\mu_1 > \mu_2 > \mu_3$. The cavity frequency is chosen to be on resonance with the $|k_1\rangle \rightarrow |k_1k_2\rangle$ transition. The effective Hamiltonian $\mathcal{H}_{\mathrm{eff}}$ that describes the couplings between the two bands in the rotating frame of the cavity field is given by

dx.doi.org/10.1021/jz501905h | J. Phys. Chem. Lett. 2014, 5, 3708−3715

$$\mathcal{H}_{\text{eff}} = \begin{pmatrix} 0 & \Omega_1 & 0 & 0 \\ \Omega_1 & \omega_{12} - \omega_c & \Omega_2 & 0 \\ 0 & \Omega_2 & \Delta_2 & \Omega_3 \\ 0 & 0 & \Omega_3 & \omega_{12} + \Delta_{23} - \omega_c \end{pmatrix} \tag{8}$$

where the frequency parameters are defined in Figure 1c. Energy is measured with respect to the lowest exciton state $|k_1\rangle$, that is, $\omega_1 \equiv 0$. For a large homogeneous aggregate, the excitonic bands become quasi-continuous, and the splittings $\Delta_2 \equiv \omega_2 - \omega_1$ and $\Delta_{23} \equiv \omega_{23} - \omega_{12}$ become negligibly small in comparison with typical line widths. Therefore, we can assume that the cavity strongly couples almost on resonance for the four levels shown in Figure 1c for large aggregates. In this regime, a weak probe field will drive transitions between the ground state $|g\rangle$ and the eigenvalues of the effective Hamiltonian $\mathcal{H}_{\text{eff}}$ in eq 8, which are the new normal modes of the cavity−matter system. In the inset of Figure 2a, we show the eigenvalues of $\mathcal{H}_{\text{eff}}$ for $\omega_c = \omega_{12}$, $\Delta_2 = \Delta_{23} = 0$, $\Omega_2 = 3\Omega_1$, and $\Omega_3 = \Omega_2/3$ as a function of $\Omega_c \equiv \Omega_2$. For $\Omega_c \ll 1$ (in arbitrary units), only three peaks can be resolved, but as Ω_c increases, the middle peak splits into a doublet, giving rise to the four-peak structure observed in the probe spectra calculated using eq 7, which includes N one-exciton states and $\sim N^2$ two-exciton states.

The number of states in the one- and two-exciton bands that couple strongly with the cavity field depends on the size of the molecular aggregate. In order to illustrate this fact, we show in Figure 2b the probe absorption spectrum for an open 1D homogeneous aggregate of size $N = 6$ without static disorder, with the same values of ω_e, J_{12}, and U_{12} and decay parameters as in Figure 2a. The cavity field is again resonant with the $|k_1\rangle \rightarrow |k_1k_2\rangle$ transition, but now, the states $|k_2\rangle$ and $|k_3\rangle$ are no longer quasi-degenerate with $|k_1\rangle$ because of the smaller array size. The cavity frequency is thus detuned from their corresponding transitions with the states $|k_1k_2\rangle$ and $|k_2k_3\rangle$ in the two-exciton band. Because the Rabi frequency Ω_3 is proportional to the transition dipole μ_{k_2,k_2k_3} by construction, whenever $\Omega_3/\Delta_{23} \ll 1$, we can set $\Omega_3 = 0$ in eq 8 to effectively remove the state $|k_2k_3\rangle$ from the excited-state dynamics. Interestingly, the eigenstates of the resulting three-level system with $\Delta_2 > 0$, plotted as a function of Ω_c in the inset of Figure 2b, show a trend in very good agreement with the microscopic model derived in eq 7.

We now include the effect of inhomogeneous disorder in the evaluation of the probe absorption spectra. In order to model static energetic disorder, we assume that the site energies are given by $\varepsilon_i = \omega_e + d_i$, where d_i is a random energy shift taken independently for each site from a Gaussian distribution with standard deviation $\sigma/|J| \approx 0.1$, consistent with the motional narrowing limit.[30,31] The susceptibility χ_p obtained from eq 7 needs to be averaged over the ensemble of disorder realizations. In Figure 3, we show the probe absorption spectrum $\mathcal{A}(\omega_p)$ of the same J-aggregates used in Figure 2a with $N = 100$ and 6 molecules, but now, static disorder is introduced in the Hamiltonian. The structure of the spectrum resembles the results in Figure 2a, but the details of the splittings near the origins are different because now the detunings Δ_2 and Δ_{23} in eq 8 are averaged over an ensemble of disorder realizations. The behavior of the outer peaks persists in the presence of disorder as a result of the strong interaction between the cavity

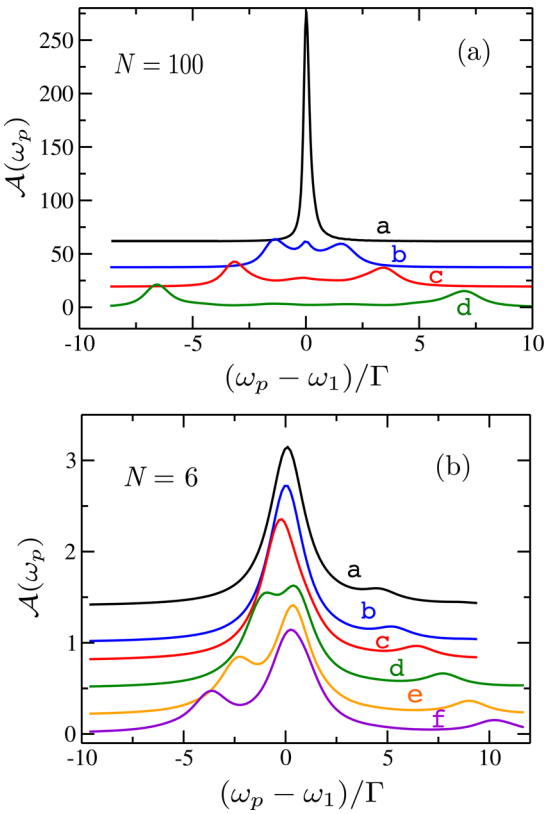

Figure 3. Probe absorption $\mathcal{A}(\omega_p)$ for a 1D J-aggregate as a function of the probe detuning from an arbitrarily chosen one-exciton state near the bottom of the one-exciton band. Dipolar couplings J_{ij} and U_{ij} are the same as those in Figure 2a. The cavity frequency is chosen such that the two-photon detuning vanishes when $\omega_p - \omega_1 = 0$. (a) The aggregate size is $N = 100$. Curves are labeled according to the mean cavity amplitudes: (a) no cavity, (b) $A_c = |\langle a \rangle| = 0.1$, (c) $A_c = 0.2$, and (d) $A_c = 0.3$. (b) The aggregate size is $N = 6$ for (a) no cavity, (b) $A_c = 0.4$, (c) $A_c = 0.8$, (d) $A_c = 1.2$, (e) $A_c = 1.6$, and (f) $A_c = 2.0$. In both panels, the vacuum Rabi frequency is $\Omega_c = \Gamma$, where $\Gamma = 26$ meV is the exciton decay rate. Static disorder is modeled by taking each monomer energy randomly from a Gaussian distribution with mean $E_0 = 2.25$ eV and standard deviation $\sigma = 0.125J$.

mode and the transition $|k_1\rangle \rightarrow |k_1k_2\rangle$, close to the deterministic resonance frequency $\omega_{12} = \omega_2 - 2|U_{12}|$.

As a final example, we consider the response of a dimer of coupled polar chromophores.[38] Clearly for $N = 2$, the bosonic approximation used in the derivation of eq 7 is no longer valid to describe the two-exciton manifold, which now consists of a single state $|e_1e_2\rangle$. However, because the structure of eqs 5 and 6 is universal, the steady-state solution for the one-exciton coherences $\mathbf{X}$ in eq 7 remains valid by simply redefining the elements of the two-photon detuning matrix $\mathbf{T}$. The one-exciton manifold has states $|\psi_+\rangle = a^{1/2}|e_1g_2\rangle + (1 - a)^{1/2}|g_1e_2\rangle$ and $|\psi_-\rangle = -(1 - a)^{1/2}|e_1g_2\rangle + a^{1/2}|g_1e_2\rangle$ with $0 \leq a \leq 1$. The transition dipole moments from the one-exciton manifold to the ground and two-exciton states are given by $\mu_\pm \equiv \langle \psi_\pm|\vec{\mu}|g_1g_2\rangle = \mu_{eg}(a^{1/2} \pm (1 - a)^{1/2}) = \langle \psi_\pm|\vec{\mu}|e_1e_2\rangle$. Given that the two-exciton energy $\omega_{12} = \epsilon_1 + \epsilon_2 - |U_{12}|$ is red shifted with respect to the one-exciton transition frequencies $\omega_\pm$, the response of a single dimer to a probe field at frequency ω_p, when the cavity is resonant with the $|\psi_+\rangle \rightarrow |e_1e_2\rangle$ transition, is given by

dx.doi.org/10.1021/jz501905h | J. Phys. Chem. Lett. 2014, 5, 3708−3715

$$\chi(\omega_p) = \mathrm{i}\left[\frac{\mu_1^2}{\epsilon_0}\right]\frac{(\Gamma_{12} - \mathrm{i}[\Delta_p + \Delta_c])}{(\mathrm{i}\Delta_p - \Gamma_1)(\mathrm{i}[\Delta_p + \Delta_c] - \Gamma_{12}) + 2D_{12}^2|A_c|^2} \tag{9}$$

which corresponds to eq 7 in the limit where **M** has a single nonzero element. Here, $\Delta_p = \omega_p - \omega_+$, $\Delta_c = \omega_c - (\epsilon_1 + \epsilon_2 + U_{12} - \omega_+)$, $\mu_1 = \mu_+$, and $D_{12} \propto \mu_+$. Γ_1 and Γ_{12} are the one- and two-exciton decoherence rates. Equation 9 shows that for coupled dimers, the cavity acts as a control for the propagation of the weak probe, in analogy with the phenomenology stemming from atomic physics to describe EIT in a cascaded three-level system.[13] Figure 4 shows the absorptive and dispersive response of an inhomogeneously broadened dimer of polar chromophores in panels a and b, respectively. The probe susceptibility has the standard features of EIT, reduction of probe absorption and steep dispersion on resonance with the lowest exciton state.[13] In comparison with atomic systems, the EIT line width for the dimer is broader even in the absence of static disorder because the two-exciton coherence is short-lived, that is, $\Gamma_{12}/\Gamma_1 \approx 1$. Inhomogeneous broadening further broadens the EIT features and, in particular, increases the absorption minimum under conditions of one and two-photon resonances $\Delta_p = 0 = \Delta_c$. For homogeneously broadened dimers (described by eq 9), the absorption minimum for a resonant probe is plotted in Figure 4c, showing a scaling of $\mathcal{A}_{\min} \approx (\Gamma_{12}/2D_{12}^2)A_c^{-2}$ for large cavity coupling $D_{12}A_c \gg \Gamma_1 \approx \Gamma_{12}$. The homogeneous curve gives a lower bound for the probe absorption minimum on resonance. The strength of the static disorder in the site basis is given by σ as before. We average over an ensemble of 1200 realizations of the site energy shifts (d_1,d_2) using an uncorrelated Gaussian joint probability distribution (JPD) of the form $P(d_1,d_2) = P(d_1)P(d_2)$. Increasing the disorder strength increases the resonant absorption of the probe $\mathcal{A}_{\min}$ for intermediate values of $D_{12}A_c$. However, as the strength of the cavity coupling increases, the homogeneous limit is recovered. This behavior has already been observed for EIT in Doppler-broadened atomic gases.[39]

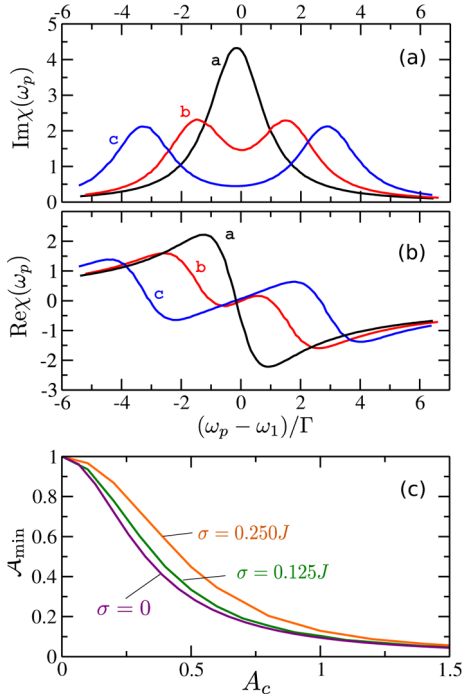

Figure 4. Im$[\chi_p]$ (a) and Re$[\chi_p]$ (b) for an inhomogeneously broadened dimer as a function of the probe detuning from the maximum of the free-space exciton absorption band. Dipolar couplings J_{ij} and U_{ij} are the same as those in Figure 2. The cavity frequency is chosen such that the two-photon detuning vanishes when $\omega_p - \omega_1 = 0$. Curves are labeled according to the mean photon number $A_c = |\langle a \rangle|$: (a) no cavity, (b) $A_c = 0.5$, and (c)$A_c = 1.0$. The vacuum Rabi frequency is $\Omega_c = 5\Gamma$, where $\Gamma = 26$ meV is the exciton decay rate. (c) Minimum absorption $\mathcal{A}_{\min}$ (normalized to the free-space value) near the deterministic resonance $\omega_p - \omega_1 = 0$ (between the Autler–Townes doublet) as a function of the mean cavity amplitude A_c. Curves are labeled by the width of the Gaussian distribution of static energy shifts σ (in units of the exchange dipole coupling J). All other parameters are the same as in those panels a and b.

In order to gain qualitative analytic understanding of the absorption minimum $\mathcal{A}_{\min}$ for inhomogeneously broadened dimers with $\sigma \neq 0$, we evaluate the mean susceptibility $\langle \chi(\omega_p) \rangle$ directly from eq 9 by averaging over an ensemble of one- and two-exciton detunings $\Delta_p = \Delta_p^{(0)} - D_p$ and $\Delta_c = \Delta_c^{(0)} - D_c$, where the random shifts (D_p,D_c) ultimately result from the site energetic disorder (d_1,d_2). We integrate over all possible shifts using $\langle \chi(\omega_p) \rangle = \int\int \mathrm{d}D_p\, \mathrm{d}D_c \chi(\omega_p,D_p,D_c)P(D_p,D_c)$, where $P(D_p,D_c)$ is the JPD for the one- and two-exciton shifts. In general, $P(D_p,D_c)$ does not factorize even if $P(d_1,d_2)$ does due to Förster coupling J_{ij}.[31] However, in order to simplify the integration over the disorder distribution, we assume an uncorrelated JPD of the form $P(D_p,D_c) = P(D_p)P(D_c)$, where $P(D) = \pi^{-2}\gamma/(\gamma^2 + D^2)$ is the Cauchy distribution with width γ. The probe absorption under conditions of deterministic one- and two-photon resonances $\Delta_p^0 = 0 = \Delta_c^0$ thus gives

$$\mathcal{A}_{\min} = \frac{\Gamma_{12} + \gamma_p + \gamma_c}{(\Gamma_1 + \gamma_p)(\Gamma_{12} + \gamma_p + \gamma_c) + 2D_{12}^2A_c^2} \tag{10}$$

where γ_p and γ_c are the widths of $P(D_p)$ and $P(D_c)$, respectively. We find that $\mathcal{A}_{\min}$ in eq 10 for a Cauchy distribution provides an upper bound for the results obtained by numerically averaging the independent site disorder over a Gaussian distribution with the same width. However, in the limit $A_c \gg (\Gamma_1 + \gamma_p)/D_{12}$, eq 10 gives $\mathcal{A}_{\min} \approx [(\Gamma_{12} + \gamma_p + \gamma_c)/2D_2^{12}]A_c^{-2}$, which tends toward the homogeneous limit for short-lived two-exciton coherences $\Gamma_{12} \gg (\gamma_p + \gamma_c)$, which is the case considered here for dimers.

In summary, we present in this Letter a general scheme to perform nonlinear optical experiments using polar J-aggregates at the single-photon level. The setup involves the use of organic chromophores with a moderate to large difference between ground- and excited-state permanent dipole moments Δd that can assemble into low-dimensional aggregate structures. We developed a theoretical model to analyze and interpret nonlinear optical signals in the regime of strong cavity–matter coupling. The constructed model is constrained within the current experimental capabilities, and we illustrate our findings using experimentally reported parameters for PIC polar dyes. The conclusions of our work are however general and go beyond our specific choice of molecular species and microcavity configuration. Organic chromophores with large permanent dipoles $d \approx 1$–10 D, both in ground and excited states, continue to be under active experimental investigation for the design of second-order nonlinear optical materials.[40−42] Upon aggregation, these polar dyes can lead to strong exciton–exciton interactions that exceed the broadening of the exciton

dx.doi.org/10.1021/jz501905h | J. Phys. Chem. Lett. 2014, 5, 3708−3715

line. For attractive interactions (J-aggregation), the cavity field can be used to strongly drive coherences between the one- and two-exciton bands without removing population from the ground state of an aggregate. Under these conditions, the absorption of a weak probe field resonant with the cavity-free exciton absorption peak is significantly modified by the presence of the cavity field containing a single photon (on average), which can be seen as quantum optical switching. In order to achieve this effect, it is important that the cavity−matter coupling exceeds all of the dissipation rates in the system, a regime that is experimentally accessible.[7,20] We have restricted our discussion to strong light−matter coupling in optical microcavities, but the strong coupling regime has also been achieved for molecular aggregates in the near-field of plasmonic nanostructures,[9,10,25] which further opens the applicability of our proposed scheme to subwavelength nonlinear quantum optics.

The ability to control molecular aggregates in optical nanostructures not only offers opportunities for the development of novel organic-based optical devices,[5] but we envision new possibilities of quantum control of excited-state dynamics relevant in energy transport and chemical reactivity and engineering of excitonic materials that are topologically robust against disorder.[43] Current experiments can achieve the regime of ultrastrong coupling with organic ensembles, where the light−matter interaction strength can be a significant fraction of the chemical binding energy.[27] In this regime, it should be possible to control the outcome of chemical reactions at the level of thermodynamics by effectively lowering reaction barriers,[44] in analogy with traditional catalytic processes, thus directly affecting reaction kinetics. This novel strong-field single-photon quantum control paradigm for molecular processes should be contrasted with traditional strong-field laser control schemes that require very high laser intensities to modify the chemical energy landscape[45] or weak-field coherent control schemes that exploit delicate laser-induced quantum interferences among internal vibronic states[46] but do not modify the energetics of the reaction. Quantum optical control of chemical dynamics is a future research direction with promising applications in nanoscience and technology, where traditional bulk methods for controlling chemical reactivity have limited efficiency.

■ ASSOCIATED CONTENT

Supporting Information

The derivation of the quantum Langevin equations leading to eqs 5 and 6 and the definition of the dynamical matrix **M** in eq 7 can be found. This material is available free of charge via the Internet at http://pubs.acs.org.

■ AUTHOR INFORMATION

Corresponding Authors

*E-mail: fherreraurbina@fas.harvard.edu (F.H.).
*E-mail: aspuru@chemistry.harvard.edu (A.A.-G.).

Notes

The authors declare no competing financial interest.

■ ACKNOWLEDGMENTS

We thank Frank Spano and Thibault Peyronel for discussions. F.H. and A.A.-G. acknowledge the support from the Center for Excitonics, an Energy Frontier Research Center funded by the U.S. Department of Energy, Office of Science and Office of Basic Energy Sciences, under Award Number DE-SC0001088. F.H., S.K.S., and A.A.G. also thank the Defense Threat Reduction Agency Grant HDTRA1-10-1-0046. B.P. and A.A-G acknowledge support from the STC Center for Integrated Quantum Materials, NSF Grant No. DMR-1231319. S.K.S. also acknowledges the support from the subsidy allocated to Kazan Federal University for performing the state assignment in the area of scientific activities. L.A.P. acknowledges support from the *Comité para el Desarrollo de la Investigación* (CODI) of the Universidad de Antioquia, Colombia under the Estrategia de Sostenibilidad 2014-2015 and from the *Departamento Administrativo de Ciencia, Tecnología e Innovación* (COLCIENCIAS) of Colombia under the Grant Number 111556934912.

■ REFERENCES

(1) Jelley, E. E. Spectral Absorption and Fluorescence of Dyes in the Molecular State. *Nature* **1936**, *138*, 1009−1010.
(2) Scheibe, G. Über die Veränderlichkeit des Absorptionsspektrums einiger Sensibilisierungsfarbstoffe und deren Ursache. *Angew. Chem.* **1936**, *49*, 563.
(3) Kobayashi, T. *J-Aggregates*; World Scientific: River Edge, NJ, 1996.
(4) Agranovich, V. M. *Excitations in Organic Solids*; International Series of Monographs in Physics; Oxford University Press: New York, 2008.
(5) Saikin, S. K.; Eisfeld, A.; Valleau, S.; Aspuru-Guzik, A. Photonics Meets Excitonics: Natural and Artificial Molecular Aggregates. *Nanophotonics* **2013**, *2*, 22−38.
(6) Würthner, F.; Kaise, T. E.; Saha-Möller, C. R. J-Aggregates: From Serendipitous Discovery to Supramolecular Engineering of Functional Dye Materials. *Angew. Chem., Int. Ed.* **2011**, *50*, 3376−410.
(7) Lidzey, G. D.; et al. Strong Exciton−Photon Coupling in an Organic Semiconductor Microcavity. *Nature* **1998**, *395*, 53−55.
(8) Coles, D.; Somaschi, N.; Michetti, P. Polariton-Mediated Energy Transfer between Organic Dyes in a Strongly Coupled Optical Microcavity. *Nat. Mater.* **2014**, *13*, 712−719.
(9) Bellessa, J.; Bonnand, C.; Plenet, J. C.; Mugnier, J. Strong Coupling between Surface Plasmons and Excitons in an Organic Semiconductor. *Phys. Rev. Lett.* **2004**, *93*, 036404.
(10) Vasa, P.; Wang, W.; Pomraenke, R. Real-Time Observation of Ultrafast Rabi Oscillations between Excitons and Plasmons in Metal Nanostructures with J-Aggregates. *Nat. Photonics* **2013**, *7*, 1−5.
(11) Zengin, G.; Johansson, G.; Johansson, P.; Antosiewicz, T. J.; Käll, M.; Shegai, T. Approaching the Strong Coupling Limit in Single Plasmonic Nanorods Interacting with J-Aggregates. *Sci. Rep.* **2013**, *3*, 3074.
(12) Scholes, G. D.; Fleming, G. R.; Olaya-Castro, A.; van Grondelle, R. Lessons from Nature about Solar Light Harvesting. *Nat. Chem.* **2011**, *3*, 763−74.
(13) Fleischhauer, M.; Imamoglu, A.; Marangos, J. P. Electromagnetically Induced Transparency: Optics in Coherent Media. *Rev. Mod. Phys.* **2005**, *77*, 633−673.
(14) Shore, B. Coherent Manipulations of Atoms Using Laser Light. *Acta Phys. Slovaca* **2008**, *58*, 243−486.
(15) Lee, K. C.; Sprague, M. R.; Sussman, B. J.; Nunn, J.; Langford, N. K.; Jin, X.-M.; Champion, T.; Michelberger, P.; Reim, K. F.; England, D.; et al. Entangling Macroscopic Diamonds at Room Temperature. *Science* **2011**, *334*, 1253−1256.
(16) Houmark, J.; Nielsen, T. R.; Mork, J.; Jauho, A.-P. Comparison of Electromagnetically Induced Transparency Schemes in Semiconductor Quantum Dot Structures: Impact of Many-Body Interactions. *Phys. Rev. B* **2009**, *79*, 115420.
(17) Akselrod, G. M.; Tischler, Y. R.; Young, E. R.; Nocera, D. G.; Bulovic, V. Exciton−Exciton Annihilation in Organic Polariton Microcavities. *Phys. Rev. B* **2010**, *82*, 113106.

(18) Schouwink, P.; Berlepsch, H.; Dähne, L.; Mahrt, R. Observation of Strong Exciton−Photon Coupling in an Organic Microcavity. *Chem. Phys. Lett.* **2001**, *344*, 352−356.
(19) Tischler, J. R.; Bradley, M. S.; Bulović, V.; Song, J. H.; Nurmikko, A. Strong Coupling in a Microcavity LED. *Phys. Rev. Lett.* **2005**, *95*, 036401.
(20) Kena-Cohen, S.; Forrest, S. R. Room-Temperature Polariton Lasing in an Organic Single-Crystal Microcavity. *Nat. Photonics* **2010**, *4*, 371−375.
(21) Kéna-Cohen, S.; Davanço, M.; Forrest, S. R. Strong Exciton−Photon Coupling in an Organic Single Crystal Microcavity. *Phys. Rev. Lett.* **2008**, *101*, 116401.
(22) Bittner, E. R.; Zaster, S.; Silva, C. Thermodynamics of Exciton/Polaritons in One and Two Dimensional Organic Single-Crystal Microcavities. *Phys. Chem. Chem. Phys.* **2012**, *14*, 3226−3233.
(23) Fofang, N. T.; Park, T.-H.; Neumann, O.; Mirin, N. A.; Nordlander, P.; Halas, N. J. Plexcitonic Nanoparticles: Plasmon−Exciton Coupling in Nanoshell−J-Aggregate Complexes. *Nano Lett.* **2008**, *8*, 3481−3487.
(24) Dintinger, J.; Klein, S.; Bustos, F.; Barnes, W. L.; Ebbesen, T. W. Strong Coupling Between Surface Plasmon−Polaritons and Organic Molecules in Subwavelength Hole Arrays. *Phys. Rev. B* **2005**, *71*, 035424.
(25) Wurtz, G. A.; Evans, P. R.; Hendren, W.; Atkinson, R.; Dickson, W.; Pollard, R. J.; Zayats, A. V.; Harrison, W.; Bower, C. Molecular Plasmonics with Tunable Exciton−Plasmon Coupling Strength in J-Aggregate Hybridized Au Nanorod Assemblies. *Nano Lett.* **2007**, *7*, 1297−1303.
(26) Sugawara, Y.; Kelf, T. A.; Baumberg, J. J.; Abdelsalam, M. E.; Bartlett, P. N. Strong Coupling between Localized Plasmons and Organic Excitons in Metal Nanovoids. *Phys. Rev. Lett.* **2006**, *97*, 266808.
(27) Schwartz, T.; Hutchison, J. A.; Genet, C.; Ebbesen, T. W. Reversible Switching of Ultrastrong Light−Molecule Coupling. *Phys. Rev. Lett.* **2011**, *106*, 196405.
(28) Chernyak, V.; Zhang, W. M.; Mukamel, S. Multidimensional Femtosecond Spectroscopies of Molecular Aggregates and Semiconductor Nanostructures: The Nonlinear Exciton Equations. *J. Chem. Phys.* **1998**, *109*, 9587−9601.
(29) Mukamel, S.; Abramavicius, D. Many-Body Approaches for Simulating Coherent Nonlinear Spectroscopies of Electronic and Vibrational Excitons. *Chem. Rev.* **2004**, *104*, 2073−2098.
(30) Knapp, E. Lineshapes of Molecular Aggregates, Exchange Narrowing and Intersite Correlation. *Chem. Phys.* **1984**, *85*, 73−82.
(31) Knoester, J. Nonlinear Optical Line Shapes of Disordered Molecular Aggregates: Motional Narrowing and the Effect of Intersite Correlations. *J. Chem. Phys.* **1993**, *99*, 8466.
(32) Spano, F. C.; Agranovich, V.; Mukamel, S. Biexciton States and Two-Photon Absorption in Molecular Monolayers. *J. Chem. Phys.* **1991**, *95*, 1400−1409.
(33) Kato, N.; Saito, K.; Aida, H.; Uesu, Y. Observations of Merocyanine J-Aggregate Domains in Mixed Molecular Monolayers using SHG/Fluorescence and Atomic Force Microscopes. *Chem. Phys. Lett.* **1999**, *312*, 115−120.
(34) Portolan, S.; Di Stefano, O.; Savasta, S.; Rossi, F.; Girlanda, R. Dynamics-Controlled Truncation Scheme for Quantum Optics and Nonlinear Dynamics in Semiconductor Microcavities. *Phys. Rev. B* **2008**, *77*, 195305.
(35) Gardiner, C. W. *Quantum Noise*; Springer-Verlag: New York, 1991.
(36) Markov, R.; Plekhanov, A.; Shelkovnikov, V.; Knoester, J. Giant Nonlinear Optical Response of Interacting One-Dimensional Frenkel Excitons in Molecular Aggregates. *Phys. Status Solidi B* **2000**, *221*, 529−534.
(37) Valleau, S.; Saikin, S. K.; Yung, M.-H.; Guzik, A. A. Exciton Transport in Thin-Film Cyanine Dye J-Aggregates. *J. Chem. Phys.* **2012**, *137*, 034109.
(38) Halpin, A.; et al. Two-Dimensional Spectroscopy of a Molecular Dimer Unveils the Effects of Vibronic Coupling on Exciton Coherences. *Nat. Chem.* **2014**, *6*, 196−201.
(39) Gea-Banacloche, J.; Li, Y.-q.; Jin, S.-z.; Xiao, M. Electromagnetically Induced Transparency in Ladder-Type Inhomogeneously Broadened Media: Theory and Experiment. *Phys. Rev. A* **1995**, *51*, 576−584.
(40) Verbiest, T.; Houbrechts, S.; Kauranen, M.; Clays, K.; Persoons, A. Second-Order Nonlinear Optical Materials: Recent Advances in Chromophore Design. *J. Mater. Chem.* **1997**, *7*, 2175−2189.
(41) Luo, J.; Zhou, X.-H.; Jen, A. K.-Y. Rational Molecular Design and Supramolecular Assembly of Highly Efficient Organic Electro-Optic Materials. *J. Mater. Chem.* **2009**, *19*, 7410−7424.
(42) Li, W.; Zhou, X.; Tian, W. Q.; Sun, X. A New Scheme for Significant Enhancement of the Second Order Nonlinear Optical Response from Molecules to Ordered Aggregates. *Phys. Chem. Chem. Phys.* **2013**, *15*, 1810−1814.
(43) Yuen-Zhou, J.; Saikin, S.; Yao, N.; Aspuru-Guzik, A. *Topologically Protected Excitons in Porphyrin Thin Films*; doi: 10.1038/nmat4073.
(44) Hutchison, J. A.; Schwartz, T.; Genet, C.; Devaux, E.; Ebbesen, T. W. Modifying Chemical Landscapes by Coupling to Vacuum Fields. *Angew. Chem., Int. Ed.* **2012**, *51*, 1592−1596.
(45) Corrales, E. M.; González-Vázquez, J.; Balerdi, G.; SoláI, R.; de Nalda, R.; Bañares, L. Control of Ultrafast Molecular Photodissociation by Laser-Field-Induced Potentials. *Nat. Chem.* **2014**, *6*, 785−790.
(46) Shapiro, M.; Brumer, P. *Quantum Control of Molecular Processes*; Wiley-VCH: New York, 2011.